Written: October 1969
Distributed: July 1971

LA-4658
UC-4, Chemistry
TID-4500

LOS ALAMOS SCIENTIFIC LABORATORY
of the
University of California
LOS ALAMOS • NEW MEXICO

The Radiolysis of Mixtures of Carbon Monoxide and Hydrogen

by

W. H. Beattie

THE RADIOLYSIS OF MIXTURES OF CARBON MONOXIDE AND HYDROGEN

by

W. H. Beattie

ABSTRACT

The self-radiolysis of mixtures of carbon monoxide (CO) and tritium ($^3H_2$) has been studied at pressures of 0.25 to 1.0 atmospheres, temperatures of -198 to +100°C, and in the presence of added H_2O or CO_2. The products of decomposition are CO_2, ^3H_2O, C^3H_4, $C_2{}^3H_4$, and a white polymer believed to be polyformaldehyde. Initial rates and G values were measured and compared with rates of ion pair formation. A mechanism for decomposition of CO and formation of products is presented. The initial rates are consistent with a mechanism involving a reaction between excited $^3H_2$ and CO to produce C^3H_4, CO_2, ^3H_2O, and a sequence of ion-molecule reactions to produce polyformaldehyde.

I. INTRODUCTION

A. Pure Carbon Monoxide

The early and recent work on the radiolysis of pure CO has been summarized, respectively, by Lind[1] and Anderson[2]. Lind and Bardwell[3] found that the two solid products, C and C_3O_2, were formed in the α radiolysis of CO. Carbon, as graphite, condensed in the gas phase and settled out while C_3O_2 condensed on the vessel walls and formed a coherent polymer film. Woodley[4] exposed CO to gamma radiation and found only one solid (composition approximately C_4O_3) formed in the gas phase. The molar ratio of carbon in the solid phase to carbon in CO_2 was approximately 4. Marsh and Wright[5] exposed CO to reactor radiation and obtained CO_2 and a polymer (composition $C_{1.9}O$). Dondes, Harteck, and Weyssenhoff[6] obtained CO and C_3O_2 polymer in the gamma radiolysis of CO admixed with a large excess (95%) of noble gas. The gas was swept free of ions with a high electrostatic field. They found that ions do not take part in the reactions. They concluded that the energy originally absorbed in the noble gas was transferred to the CO, forming excited CO species that react with normal CO molecules, producing the products.

A detailed investigation was made by Anderson, Best, and Willett[7] using proton radiolysis with a flow technique to eliminate possible reactions with the products. They analyzed the solid polymer without prior exposure to air and showed that the stoichiometry is given by $4CO = CO_2 + C_3O_2$. Increasing the temperature from 20 to > 450°C resulted in a solid, richer in carbon. This was attributed to secondary pyrolysis of the carbon suboxide polymer forming C and CO_2. The yield, $G(CO_2)$, obtained at low dose rates was 1.96. This is in good agreement with their value of 2.05 obtained with proton radioloysis, 2.3 obtained by Johnson, and 1.9 obtained by Dondes. Using 1.9 for $G(CO_2)$, their stoichiometry gives a value of 8 for $G(-CO)$ in good agreement with the range of values 8.4 to 9.6 given by Rudolph and Lind.[1] An error in Lind's earlier range of values, 12 to 20, was attributed to traces of O_2, which Anderson, et al.[7] showed would increase yields significantly.

At high dose rates, yields are significantly decreased. In order to explain this effect, Anderson, et al.,[7] proposed the following reaction mechanism:

$$CO \rightsquigarrow CO^+ + e^- \qquad (1)$$

$$CO \rightsquigarrow CO^* \qquad (2)$$

$$CO^+ + e^- \rightarrow CO^* \rightarrow C + O \qquad (3)$$

$$CO^+ + CO \rightarrow (CO)_2^+ \xrightarrow{CO} (CO)_n^+ \qquad (4)$$

$$(CO)_n^+ + e^- \rightarrow n\ CO \qquad (5)$$

$$CO + O \rightarrow CO_2 \qquad (6)$$

$$CO + C \rightarrow C_2O \qquad (7)$$

$$C_2O + CO \rightarrow C_3O_2 \qquad (8)$$

$$C_2O + O \rightarrow 2\ CO \qquad (9)$$

While insignificant at low dose rates, Reaction (9) predominates over Reaction (6), at high dose rates causing the yield to be decreased. Using the finding of Dondes, Harteck, and Weyssenhoff[6] (that the rate is controlled primarily by the reaction of excited, rather than ionized, CO molecules) Anderson, Best, and Willett[7] were able to explain the inefficient utilization of energy by CO. Therefore, they postulated that Reaction (3) was of minor importance compared to Reactions (4) and (5).

Blake and Hodgson[8] showed that the polymerization of carbon suboxide, C_3O_2, by gamma radiation, releases small quantities of CO. They found $G(-C_3O_2) = 2900$ to 5200 whereas $G(CO) = 39$ to 50. To account for the high G values, an ionic-chain mechanism, initiated by C_2O^+ or $C_3O_2{}^+$, was proposed.

Recent work by Willis and Devillers,[9] who spectrometrically identified $C_2O(^3\Sigma)$ and long-lived $C(^1S)$ as products of the pulse radiolysis of CO, requires modification of Anderson's scheme. Reaction (7) is eliminated because the long lifetime found for C atoms shows that they are not the exclusive precursors of C_2O. Willis and Devillers also argued that CO^+ cannot be a percursor of C_2O, and showed that formation of C_2O by Reaction (7′) is possible if the energy contained in the excited state ≥ 8.9 eV.

$$CO^* + CO \rightarrow C_2O(^3\Sigma) + O(^3P) \qquad (7')$$

Thus, Reaction (7′) should replace (7). This reaction, originally suggested by Dondes, Hartek, and Weyssenhoff[6] was included as an alternate mechanism by Anderson, Best, and Willett.[7] Additional support for this mechanism was given in a study of the gamma radiolysis of CO by Briggs and Clay[10] who determined that the yield of $O(^3P)$ could account for 75% of the yield of CO_2, and concluded that ionic reactions are not involved in the formation of $O(^3P)$ atoms. They postulated that the remaining yield of CO_2 was formed by the reaction $CO^* + CO \rightarrow CO_2 + C$.

Baulch, Drysdale, and Lloyd[11] have suggested that the recombination of CO and O requires a third body, as follows:

$$O + CO + M \rightarrow CO_2 + M \qquad (6')$$

Experiments on the effects of walls upon the electrical discharge decomposition of CO_2[12] support the mechanism of Reaction (6′) in preference to Reaction (6).

The simplest mechanism of decomposition during the radiolysis of pure CO, in agreement with these combined findings and Anderson's stoichiometry, is given by Reactions (2), (7′), (6′), and (8), followed by polymerization.

B. Mixtures of Carbon Monoxide and Hydrogen

The reaction mechanism in the radiolysis of mixtures of CO and H_2 is considerably more complex than for pure CO. Early work by Lind,[1,3] using radon, indicated that equimolar mixtures of CO and H_2 formed a white insoluble solid of empirical composition $C_{1.64}H_5O$. Douglas[13] mixed CO with $^3H_2$, in slight excess, and allowed self-radiolysis. The products, identified mass spectrometrically, were: ^3H_2O, CO_2, acetaldehyde, glycol, glyoxal, and a white solid identified as polyformaldehyde. Moseley, Truswell, and Edwards[14] irradiated mixtures of CO and H_2 with fission fragments released from thin films containing ^{235}U and obtained, as products, CO_2 and small quantities of CH_4 and CH_2O. They found that $G(CO_2)$ increased with the fraction of CO and reached a maximum value of 1.4 for pure CO. Mikhailov, Kiselev, and Bogdanov[15] irradiated various mixtures of CO and H_2 with 115 keV electrons and obtained CO_2 glyoxal, acids, CH_2O, and (in experiments with low H_2 content) carbon suboxide polymer, and found that the decomposition rate and yields varied with composition.

Since previous work on the CO - H_2 system is fragmentary and lacks definitive interpretations, it was clear that a more comprehensive study of radiolysis of the CO - H_2 mixture was needed. This work is a study of the self-radiolysis and reaction kinetics of the CO-$^3H_2$ system in the range 3 to 33% CO. The nomenclature used here is the same as given in Ref. 16.

II. EXPERIMENTAL

Matheson CP-grade CO, containing ~ 0.1% each of O_2 and CO_2, was used without purification. Isotopic $C^{18}O$ enriched to 99.7% ^{18}O, and containing 2.0% other impurities (primarily $^{15}N_2$), was prepared at this laboratory. Isotopically enriched $^3H_2{}^{18}O$, was prepared by reacting $N^{18}O$ with $^3H_2$ under self-radiolysis, and pumping off impurities three times at -80°C, following temperature cycles to 25°C.

Experimental details describing the other gases used, the apparatus, procedures for filling, and methods of analysis are given in Ref. 16, with the following exception: gases were filled in the order, CO_2 or H_2O, CO, $^3H_2$. Since CO cannot be frozen in the cold finger with liquid N_2, the $^3H_2$ was added to the previously filled gaseous CO (and frozen CO_2 or H_2O, when used), and the reaction bulb quickly closed. The combined pressure of CO and $^3H_2$ was measured and their partial pressures calculated from subsequent mass spectrometric analysis.

III. RESULTS

The major products obtained by self-radiolysis of mixtures of CO and $^3H_2$ were CH_4, H_2O, and a white polymeric solid. Small quantities of CO_2, C_2H_4, and traces of CH_2O and some unidentified compounds (possibly including H_2O_2 and C_2H_2) were found.

The variation of the mole fraction of CO and other measurable gaseous products formed during a typical experiment are shown in Fig. 1. Smooth curves were obtained by using a computer to obtain and plot a least-squares fit of data points to a cubic spline. The mole fraction of $^3H_2$ is not shown because the mass spectrometric analysis was not sufficiently accurate. A

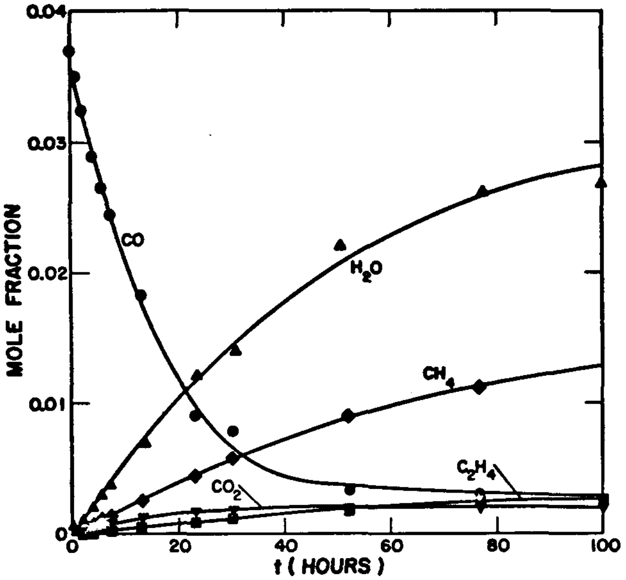

Fig. 1. Variation of mole fractions of CO, CO_2, CH_4, C_2H_4, and H_2O during a typical experiment (Run 31). All curves were smoothed using a computer program.

low concentration of O_2 could always be detected, increasing from the initial value to a steady value of ~ 0.1% during approximately the first 10 hours. Most of the decomposition of CO and formation of products occurred during the first two days of reaction. After 2 to 4 weeks, the partial pressure of CO reached a low steady-state value.

Plots of log P_{CO} versus time are initially nearly linear, but the slope eventually decreases as shown in Fig. 2. Thus, the overall decomposition rate of CO would appear to be first order with respect to CO with a superimposed back reaction appearing as product concentrations build up. However, the kinetics of the decomposition of CO is complicated because three major carbon-containing products, CO_2, CH_4, and polymer, are formed from CO. The kinetic law governing the decomposition of CO is the sum of the kinetic laws for the formation of the three products.

In each experiment the initial rate was measured using the first 4 to 6 points of each curve in plots such as Fig. 1. The

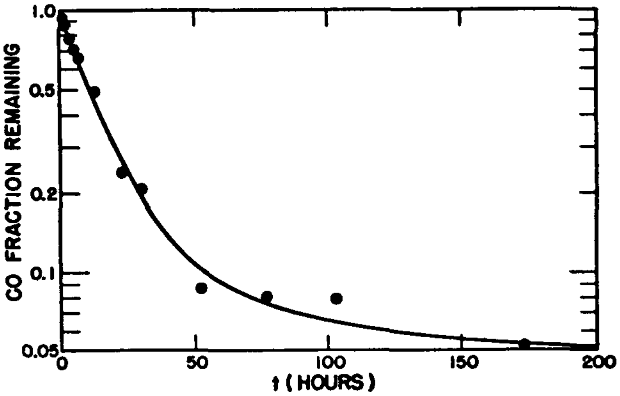

Fig. 2. Fraction of CO vs time, for the experiment shown in Fig. 1, testing for first-order kinetics.

initial pressures and temperatures, initial rates of disappearance of reactants, and initial rates of appearance of products are summarized in Table I. Table I also includes the rates of ion-pair formation for CO^+ and $H_2{}^+$, which were calculated as described in Ref. 16.

For the purpose of comparing this work with others, the yields have been calculated from the initial rates [16] and are listed in Table II. Yields obtained over longer time spans would be lower than the values listed hence would be of no significance.

The role of surface area was tested by etching the inside of one reaction bulb with HF. Comparison of Runs 33 and 34 shows that the initial rates agree, within experimental error, despite the difference in surface area. Plots of mole fraction of CO vs time are almost identical for these runs. It is concluded that the surface area of the bulb has no detectable effect upon the reaction kinetics.

In Runs 23 and 26, ${}^3H_2{}^{18}O$ was added to the $C^{16}O$ - ${}^3H_2$ mixture so that the $C^{16}O^{18}O$ formed from $C^{16}O$ plus ${}^3H_2{}^{18}O$ could be distinguished from the $C^{16}O_2$ formed from $C^{16}O$ alone. The rates of CO and CO_2 formation are listed in Table III.

In Runs 24 and 25, the decomposition kinetics of mixtures of CO, CO_2, and ${}^3H_2$ were investigated. Double isotopic labeling

TABLE I. Initial Experimental Conditions and Initial Rates for the Radiolysis of Mixtures of CO and H_2

		Initial Pressure, (torr)			Measured Initial Rates, (torr/h) x 10^2						Calculated Initial Rates, (torr/h) x 10^2	
Run No.	Temp, °C (1)	P_{H_2} (2)	P_{CO}	P_i (3)	$-\frac{dP_{CO}}{dt}$	$\frac{dP_{CO_2}}{dt}$	$\frac{dP_{CO}}{dt}$	$\frac{dP_{CH_4}}{dt}$	$\frac{dP_{H_2O}}{dt}$	$\frac{dP_{C_2H_4}}{dt}$	$\frac{dP_{CO^+}}{dt}$	$\frac{dP_{H_2^+}}{dt}$
3	ambient	412.6	11.5		60.	3.6		5.35	17.5		10.9	60.7
19	"	184.0	12.6	17.2 (H_2O)	57.	14.2		——			7.19	15.8
20	"	192.0	11.0		24.4	1.46		3.39			8.14	21.5
21	-80	187.0	11.0		21.5	< 0.6		3.32			8.04	20.7
22	-198	163.0	11.0		16.4	~ 0.3		2.9			7.06	17.2
23	ambient	203.7	19.6	10.1 (H_2O)	38.9	8.12 (4)	4.43 (4)	3.56	26.0		12.0	18.8
24	"	170.6	15.09	10.15 (CO_2)	24.3 (5)	6.02 (6)	13.6 (6)	2.67 (6)		1.57 (6)	7.91	13.5
25	"	182.6	1.53	20.34 (CO_2)	10.43 (5)	3.1 (6)	16.1 (6)	1.04 (6)		0.06 (6)	0.81	14.6
26	"	211.0	50.0	21.0 (H_2O)	77.	17.4 (4)	7.51 (4)	3.43		——	22.3	14.3
27	"	194.4	29.6		33.4	4.17		3.76	9.32	0.69	17.0	16.9
28	"	211.8	108.2		47.0	8.83		2.94	8.51	0.55	31.4	9.32
31	"	524.5	19.1		113.6	4.97		11.18	27.6	1.94	19.3	73.0
32	"	505.7	37.9		130.	8.10		9.10	24.8	1.51	30.1	60.9
33	"	276.1	13.8		38.9	3.06		5.39		1.28	11.3	36.2
34 (7)	"	276.1	13.9		34.9	3.30		5.32		1.16	11.3	36.1
35	-40	319.3	15.1		31.9	2.12		6.57		0.77	12.5	40.7
36	+100	192.9	14.4		14.4	5.64		4.05		0.95	10.0	20.5

TABLE I NOTES

1. Ambient temperature, ~ 22°C. Temperature in Runs 21 and 22 refers to the cold finger with bulb at ambient temperature.
2. Pressures of H_2 include all isotopes. Gas purity ~ 98% $^3H_2$, 1.7% $^2H_2$, and 0.3% $^1H_2$.
3. In Runs 23 and 26, $^3H_2{}^{18}O$ was used; in Run 19 ordinary water was used.
4. In Runs 23 and 26, the rate formation of CO_2 includes the sum of $C^{18}O_2$ and $C^{16}O^{18}O$, and dP_{CO}/dt is for the $C^{18}O$ isotope. See Table III for isotopic rates.
5. In Runs 24 and 25, $^{12}C^{18}O$ and $^{13}C^{16}O_2$ were used. Rates of decomposition refer to these isotopes only. A summary is given in Table IV.
6. In Runs 24 and 25, the rates dP_{CO_2}/dt are given for the sum of $^{12}C^{16}O^{18}O$ and $^{12}C^{18}O_2$, and dP_{CO}/dt are given for the sum of $^{13}C^{16}O$ and $^{12}C^{16}O$. The initial rates of formation of $^{12}C\,{}^{16}O_2$ and $^{13}C^{18}O$ were zero. The rates dP_{CH_4}/dt and $dP_{C_2H_4}/dt$ are for the compounds $^{12}C^3H_4$ and $^{12}C_2{}^3H_4$. The initial rates of formation of $^{13}C^3H_4$ and $^{13}C_2{}^3H_4$ were zero.
7. The surface area of the bulb in Run 34 was increased by etching with aqueous HF. The etched surface was slightly translucent but sufficiently transparent to see clearly into the interior.

TABLE II. Experimental Values of Yields Calculated from Initial Rates.

Run No.	G(-CO)	G(CO_2)	G(CH_4)	G(H_2O)
3	2.3	0.14	0.20	0.67
20	2.3	0.14	0.32	——
21	2.1	<0.06	0.32	——
22	1.9	0.03	0.33	——
23	4.4	0.91	0.40	2.9
26	5.1	1.1	0.22	——
27	2.8	0.35	0.31	0.77
28	3.3	0.63	0.21	0.60
31	3.4	0.15	0.33	0.82
32	4.0	0.25	0.28	0.76
33	2.3	0.18	0.31	——
34	2.0	0.19	0.31	——
35	1.7	0.11	0.34	——
36	1.3	0.51	0.37	——

TABLE III. Isotopic Initial Rates for Runs with H_2O Added to the Mixture of CO_2 and H_2

		Initial Rates, (torr/h) x 10^2		
	Rate Expression	Run 19	Run 23	Run 26
1.	$dP_{C^{18}O_2}/dt$		3.85	7.4
2.	$dP_{C^{16}O^{18}O}/dt$		4.27	10.0
3.	Sum of 1 and 2	14.2	8.12	17.4
4.	$dP_{C^{18}O}/dt$		4.43	7.51
5.	Sum of 2 and 4		8.7	17.5
6.	$dP_{H_2O^+}/dt$	6.42	4.07	6.18

using $^{12}C^{18}O$ and $^{13}C^{16}O_2$ made possible the identification of both C and O in the products from either the CO or the CO_2. The initial rates of formation of $^{12}C^{16}O_2$ and $^{13}C^{16}O^{18}O$ were zero, within experimental error, indicating that carbon does not exchange directly between CO and CO_2, and that oxygen in the CO_2 does not exchange with oxygen from CO (although oxygen from CO_2 does react with CO).

The initial rates of formation of the only significant products of isotopic CO and CO_2 are given in Table IV. The rate of disappearance of CO_2 is approximately equal to the rate of ionization of CO_2 in agreement with the rate in the absence of CO (as shown in Ref. 16). The isotopically unlabeled initial rates are given in Table I. Those rates also represent the sum of the rates of the labeled products.

The stoichiometry of Runs 24 and 25 was clarified by plotting the mole fractions of products $^{12}C^{16}O^{18}O$ and $^{12}C^{16}O$ vs the mole fraction of the $^{13}C^{16}O_2$ reactant remaining. The limiting initial slopes give the fraction of CO_2 converted to each product (Table IV). Within experimental error, the sum of the fractions is equal to 1.0, indicating that essentially all of the ^{16}O from decomposing $^{13}C^{16}O_2$ reacts with the $^{12}C^{18}O$.

During the first 10 to 50 hours of CO decomposition, a minor peak grew at a mass-to-charge ratio of 31 (m/e 31). The rate of growth was greater with high concentrations of CO. After several days the peak decreased and eventually disappeared. The peak at m/e 31 corresponds to the formyl radical, C^3HO. In Run 26, originally containing $^3H_2{}^{18}O$ and $C^{16}O$, peaks at m/e 31 and m/e 33 (corresponding to $C^3H^{16}O$ and $C^3H^{18}O$) grew at approximately the same rate. This could occur only if the rate of isotopic exchange were fast.

In Run 29, $^3H_2$ was mixed with the vapor from aqueous formaldehyde (methanol-stabilized). Within minutes after mixing, turbidity appeared, indicating a very rapid formation of polymer. The partial pressure of CH_2O was determined from the parent peak at m/e 30. The rate of disappearance of CH_2O was much faster than the calculated rate of ion-pair formation (see Table V). Only a small fraction of the disappearing C^1H_2O was converted to C^1H^3HO. Growth of the peak at m/e 28 indicated probable conversion of some formaldehyde to CO, but interference from C^1H_2O fragments made analysis impossible.

TABLE IV. Summary of Runs with CO_2 Added to the Mixture of CO and H_2.

		Fraction of Original $^{13}C^{16}O_2$	
		Run 24	Run 25
1.	$^{12}C^{16}O^{18}O$ formed from $^{13}C^{16}O_2$	0.39±0.06	0.19±0.10
2.	$^{12}C^{16}O$ formed from $^{13}C^{16}O_2$	0.67±0.3	1.2 ±0.5
3.	Sum of 1 and 2	1.06±0.4	1.4 ±0.6

		Initial Rates, (torr/h) x 10^2	
	Rate Expression	Run 24	Run 25
4.	$dP_{^{12}C^{16}O^{18}O}/dt$	2.98	1.9
5.	$dP_{^{12}C^{16}O}/dt$	6.6	6.
6.	Sum of 4 and 5	9.6	7.9
7.	$dP_{^{13}C^{16}O}/dt$	7.0	10.1
8.	$dP_{^{12}C^{16}O_2}/dt$	3.04	1.2
9.	$dP_{^{13}C^{16}O_2^+}/dt$ (calculated)	8.29	16.7
10.	$dP_{^{12}C^{16}O^+}/dt$ (calculated)	7.91	0.81
11.	$-dP_{^{12}O^{16}O_2}$ /dT	5.88	12.74

TABLE V. Initial Pressures and Rates for Run 29, Containing Aqueous CH_2O (Methanol-Stabilized) and $^3H_2$.

P_{CH_2O}	7.06 torr
$P_{^3H_2}$	40.6 torr
$-dP_{CH_2O}/dt$	0.456 torr/hr
$dP_{CH_2O^+}/dt$	0.003 torr/hr
$dP_{^3H_2^+}/dt$	0.16 torr/hr

The white polymeric solid was formed in all runs. In runs without initial H_2O, the polymer became apparent as faint turbidity a few hours after the gases were mixed, and became opalescent slowly. During the first half-day of reaction, illumination of the aerosol with a beam of white light produced a higher-order Tyndall spectra,[17] indicating the presence of highly monodisperse particles estimated to be ~ 0.2 microns in diameter. During the first day, the particles settled on the bottom of the reaction bulb as a white powder. After several days, the powder was transformed into a translucent film. Polymer was formed in the gas phase during only approximately the first day of a run. In runs with H_2O included in the mixture, most of the polymer was deposited initially on the surface as a translucent film.

The concentration of polymer could not be measured directly, but was determined from material balance. In Fig. 3 the mole fraction C and the mole fraction O contained in the gases in the bulb are plotted for comparison with the mole fraction CO. The mole fraction of C or O that is converted to polymer is the difference between the mole fraction at zero time and the mole fraction at some later time. Figures 1 and 3 show that most of the O, and a small fraction of the C, deposited in the original polymer are later converted to H_2O and CH_4.

The initial rate of formation of the polymer increased with the partial pressure of $^{3}H_2$. At equivalent pressures, the rates at low temperatures were approximately the same as those at 23°C, but the rate at 100°C was less than one-fifth of the rate at 23°C. The total amount of polymer formed during an experiment, i.e., from the beginning until all rates approached zero, was greatest in the low-temperature runs, and considerably less at 100° than at 23°C.

The final polymer film was insoluble in water, acetone, methanol, normal hexane, and trichloroethylene. It did not detectably decompose after several minutes heating the bulb with a 260°C heat gun.

The variation of mole fractions of CO_2, CH_4, and C_2H_4 are shown in detail in Fig. 4. The rates of formation of CH_4 and C_2H_4 are approximately proportional to each other during an experiment.

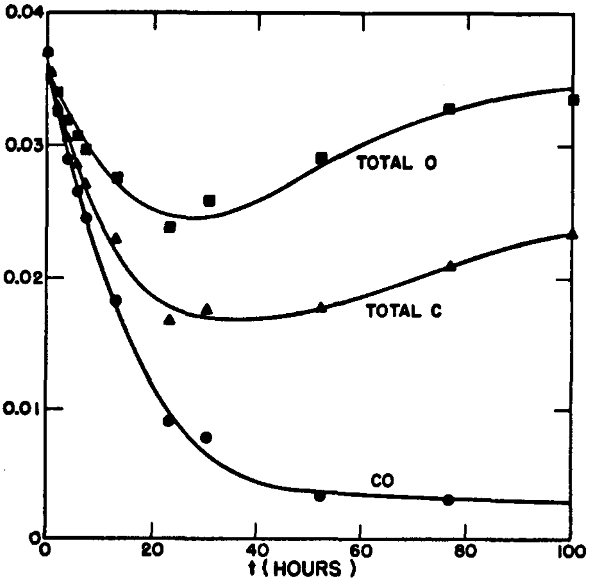

Fig. 3. Variation of the total mole fractions of carbon and oxygen in the gas phase, and mole fraction of CO (Run 31). The decreasing mole fractions of carbon and oxygen correspond to formation of polymer. Curves were smoothed using a computer program.

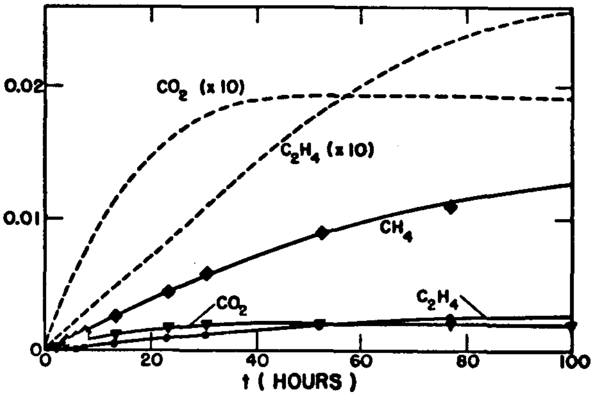

Fig. 4. Variation of mole fractions of CH_4, C_2H_4, and CO_2 during a typical experiment (Run 31), and with a 10-fold scale expansion of the ordinate for C_2H_4 and CO_2. Curves were smoothed using a computer program.

Comparison of Figs. 1, 3, and 4 shows that the rates of formation of CO_2 and polymer decrease to zero at approximately the time when the partial pressure of CO decreases to a low value near its steady-state value, but the formation of CH_4, C_2H_4, and H_2O continue to increase after this time.

IV. DISCUSSION

A. Reaction Scheme

The $CO-H_2$ system under radiolysis undergoes a surprisingly great number and variety of reactions. The complexity of the system frustrates a straightforward interpretation of data. To clarify this discussion, a reaction scheme will be presented first and the evidence supporting it will be given later. The following sequence of reactions describe the decomposition of CO into polymer, CH_4, H_2O, and CO_2. The reactions were selected by considering all known reactions between the species present, eliminating as many reactions as possible upon thermodynamic or kinetic grounds, and selecting reactions from the remainder which are compatible with experimental results.

$$H_2 \rightsquigarrow H_2^+ + e^- \tag{10}$$

$$H_2 \rightsquigarrow H_2^* \tag{11}$$

$$CO \rightsquigarrow CO^+ + e^- \tag{12}$$

$$H_2^* + H_2 \rightarrow 2H_2 \tag{13}$$

$$H_2^* + CO \rightarrow CH + OH \tag{14}$$

$$H_2^* + CO \rightarrow C + OH + H \tag{15}$$

$$CH + H_2 \rightarrow CH_3 \tag{16}$$

$$CH_3 + H_2 \rightarrow CH_4 + H \tag{17}$$

$$H_2^+ + H_2 \rightarrow H_3^+ + H \tag{18}$$

$$H_2^+ + CO \rightarrow CO^+ + H_2 \tag{19}$$

$$H_3^+ + CO \rightarrow CHO^+ + H_2 \tag{20}$$

$$CO^+ + H_2 \rightarrow CHO^+ + H \tag{21}$$

$$CHO^+ + e^- \rightarrow CHO^* \tag{22}$$

$$CHO^* + H_2 \rightarrow CH_2O + H \tag{23}$$

$$CHO^+ + e^- \rightarrow CO + H \tag{24}$$

$$CH_3 + CH_3 \rightarrow C_2H_6^* \rightarrow C_2H_4 + H_2 \tag{25}$$

$$OH + H_2 \rightarrow H_2O + H \tag{26}$$

$$OH + CO \rightarrow CO_2 + H \tag{27}$$

$$H + H + M \rightarrow H_2 + M \tag{28}$$

The total sequence of reactions, including reactions of the products and the above reactions, are summarized in reaction flow diagrams, with conservation of carbon, oxygen, and hydrogen in Fig. 5. The reactions of CO_2 and those producing CO_2 have

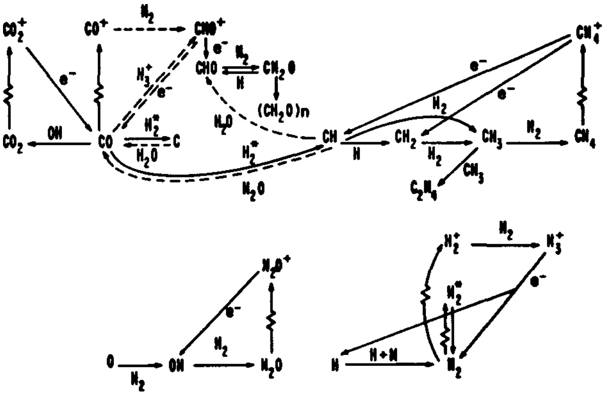

Fig. 5. Reaction flow diagrams for the $CO-H_2$ system. Reactants are shown at the beginning and side of each arrow, and the products of interest at the end. Carbon is conserved in upper diagram, and oxygen and hydrogen in lower diagrams. Zigzag lines indicate radiolysis, and dashed lines indicate reactions with little supporting evidence.

been discussed in Ref. 16. On each diagram the more-oxidized species are on the left and the more-reduced species on the right. Higher-energy species are generally on the upper part of the diagram. Dashed lines indicate plausible reactions for which little or no experimental evidence exists.

The arrows flowing out from CO and H_2 indicate possible initial-reaction paths. The total network of arrows represents the eventual state of dynamic equilibria that interact to produce steady-state pressures of many species.

B. Formation of CH_4

In runs with initial gas mixtures of only CO and $^3H_2$, the rate of formation of CH_4 was approximately constant, and, as the partial pressure of CO decreased to 1 to 4 torr, the rate of forming CH_4 decreased to zero, (see Fig. 1). The values of the initial rate of formation of CH_4 given in Table I are almost the same, although the initial pressures of CO vary over a wide range. Therefore, the rate of formation of CH_4 is essentially independent of the pressure of CO if the pressure is not too low. The same phenomenon was observed in experiments containing initially only CO_2 and $^3H_2$.[16] Here the rate of formation of CH_4 increased from zero with the pressure of CO and became constant when the pressure of CO exceeded a value of 0.3 to 1.4 torr.

In the experiments containing both $C^{18}O$ and $^{13}CO_2$ (Runs 23 and 24), the initial rates of formation $^{13}C^3H_4$ were zero while the initial rates of formation of $^{12}C^3H_4$ were high. This confirms the data in Ref. 16 which indicates that CH_4 is not formed directly from CO_2.

Comparison of the rates with and without added H_2O or CO_2 (Table I), indicates that the rate of formation of CH_4 is unaffected by the presence of H_2O or CO_2. The agreement among the values of the rate of formation of CH_4 in Runs 20, 21, and 22, indicates that it also is independent of temperature. This temperature independence is also found in the relationship shown in Fig. 6, and was observed during the decomposition of CO_2.[16]

The temperature independence of the rate of formation of CH_4 indicates that the rate-controlling step is probably excitation or ionization resulting from radiolysis. However, it is unlikely that CH_4 is formed from either excited CO or CO^+ ions, because the measured initial rates of formation of CH_4 are unrelated to the calculated rates of formation of CO^+ ions. On the other hand, the initial rate of formation of CH_4 is directly related to the rate of formation of H_2^+ and the ratio of P_{H_2}/P_{CO} as shown in Fig. 6 and given by the linear relationship between $(dP_{H_2^+}/dt)/(dP_{CH_4}/dt)$ (or simply $dP_{H_2^+}/dP_{CH_4}$) and P_{H_2}/P_{CO} in Eq. (29). The constants and standard deviations were determined by a least-squares fit of the data points to the line.

$$\frac{dP_{H_2^+}}{dP_{CH_4}} = (0.138 \pm 0.022)\left(\frac{P_{H_2}}{P_{CO}}\right) + (3.7 \pm (.3) \qquad (29)$$

Next it will be shown that the reaction scheme is compatible with this rate law.

It is unlikely that atomic C is an intermediate in the mechanism forming CH_4, because the reaction $C + H_2 \rightarrow CH + H$ is slow for ground state C,[18] and C reacts with many oxygen-containing molecules to produce CO.[19] The radical CH can be an intermediate, since Reaction (16) is rapid.[20]

The proportionality between the rates of formation of CH_4 and H_2^+ indicates that the rate-controlling step in forming CH_4 is a reaction between CO and a species derived from the energy absorbed in H_2. The reacting species is probably not H_2^+ because Reaction (18) is rapid,[21] making its concentration low. This is supported by Coulter, Leckey, and Higginson,[22] who measured the hydrogen ions present in a low

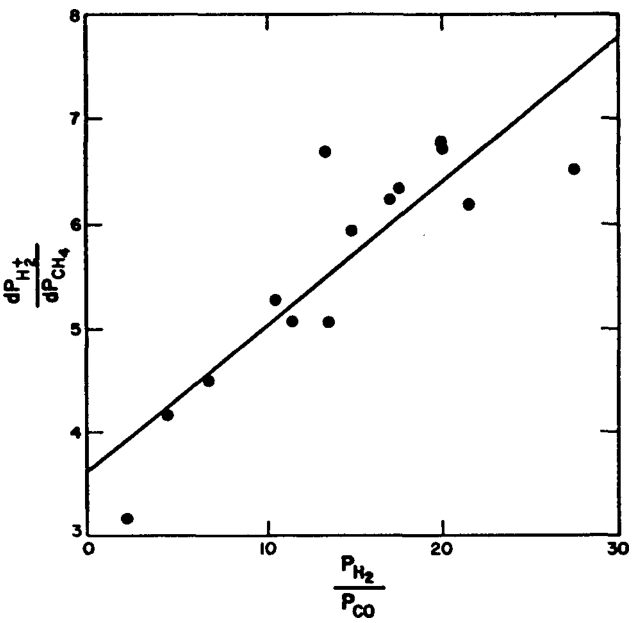

Fig. 6. The ratio of the calculated rate and formation of H_2^+ to the measured initial rate of formation of CH_4 vs the ratio of the pressure of H_2 to CO. The straight line is a least-squares fit of data points. Runs 3 and 25 are not included.

voltage arc at an H_2 pressure of 0.3 torr, and found 99% H_3^+, 1% H^+, and no H_2^+. Reactions between H_3^+ and CO cannot produce CH^+ or CH_2^+ because of high positive $\Delta H°$. Instead, Reaction (20) is postulated. Recombination of CHO^+ with an electron could produce CH + O, but it is energetically more favorable to produce CO + H or CHO (Reactions (22) or (24).) Thus it seems unlikely that reactions of hydrogen ions or their derivatives with CO can produce CH, CH_2, or CH_3.

The activation energies for the reactions H + CO → CH + O and H_2 + CO → CH + OH are estimated by Otozai's rule[23] to be 51 and 103 kcal/mole respectively, which means that only hot H atoms or the excited species, H^* and H_2^*, have sufficient energy to react rapidly with CO. Reactions with either hot or excited H atoms are improbable because both the estimated number of collisions between hot H and CO, and the number of H^* formed per H_2^+, are too low to account for the observed rate of formation of CH_4. The number of H_2^* formed per H_2^+ in pure $^3H_2$ has been estimated by *W. M. Jones*[24] to be 0.8 singlet states and 0.6 triplet states. Since singlet states are quenched by H_2, it will be assumed that CH_4 is formed primarily from triplet H_2^* by Reactions (14), (16), and (17).

Reactions (16) and (17) are fast[20, 25] with respect to the rate expected for Reaction (14); therefore their rates are independent of P_{H_2} when $P_{H_2} >> P_{CH}$. Therefore, Reaction (14) is assumed to be rate-determining and equal to R_{16} and R_{17}. At a steady-state pressure of H_2^*, R_{11} is equal to $R_{13} + R_{14} + R_{15}$, and the usual treatment yields:

$$P_{H_2}{}^* = \frac{R_{11}}{k_{13}\,P_{H_2} + k_{14}\,P_{CO} + k_{15}\,P_{CO}} . \qquad (30)$$

Substituting $P_{H_2}{}^*$ into R_{14}, R_{17} for R_{14}, and 0.6 R_{10} for R_{11} yields, upon rearrangement:

$$\frac{0.6\,R_{10}}{R_{17}} = \frac{k_{13}\,P_{H_2}}{k_{14}\,P_{CO}} + \left(1 + \frac{k_{15}}{k_{14}}\right) . \qquad (31)$$

This is identical in from to Eq. (29), which gives the values 0.138 for k_{13}/k_{14} and 1.7 for k_{15}/l_{14}.

This mechanism accounts only for initial rates of formation of CH_4. It does not consider CH_4 which is formed late in the reaction by decomposition of the polymer.

C. Formation of C_2H_4

It has been well established[26] that C_2H_4 is the most abundant product, other than hydrogen, produced by the radiolysis of pure methane. In the mechanism postulated by Rudolph,[26] CH_4^+ ions react forming CH_3 radicals, which then react according to Reaction (25).

In this work, C_2H_4 is not a product of decomposition of CH_4, because the rate for formation of C_2H_4 is not proportional to the concentration of CH_4 (Fig. 3). It may, however, be assumed that CH_3 radicals produced by Reaction (16) will react by Reaction (25). Consequently Reactions (17) and (25) will compete, and the rates of formation of CH_4 and C_2H_4 will be related, as observed.

D. Formation of CO_2

Examination of Table I shows that the initial rate of formation of CO_2 is not related to the rate of formation of CO^+ ions. As with the formation of CH_4, the formation of CO_2 does not depend upon the ionization of CO.

The kinetics of formation of CO_2 were found to be somewhat analogous to the kinetics of formation of CH_4. A linear relationship between $(dP_{H_2^+}/dt)/(dP_{CO_2}/dt)$ and P_{H_2}/P_{CO} is shown in Fig. 7 and given by Eq. (32). The constants and standard deviations were determined by a least-squares fit of the data points to the line.

$$\frac{dP_{H_2^+}}{dP_{CO_2}} = (0.50 \pm 0.06)\left(\frac{P_{H_2}}{P_{CO}}\right) + (0.87 \pm 1.2) \qquad (32)$$

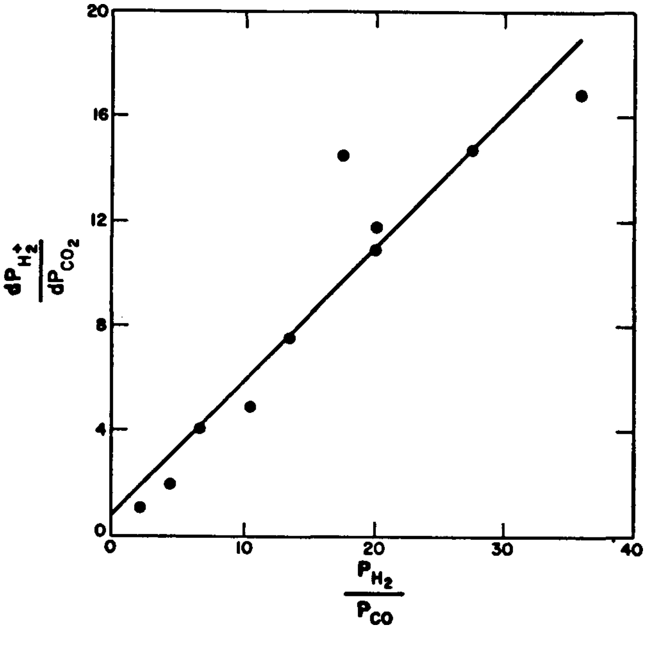

Fig. 7. The ratio of the calculated rate of formation of H_2^+ to the measured initial rate of formation of CO_2 vs the ratio of the pressure of H_2 to CO for runs at ambient temperature. The straight line is a least-squares fit of date points. Runs 19, 24 and 25 are not included.

As in the kinetics of forming CH_4, the rate-controlling step is evidently a reaction between CO and a species derived from the energy absorbed in H_2, e.g., H_2^+ or H_2^*.

The rate of formation of CO_2, unlike that of CH_4, was increased by the addition of H_2O vapor to a mixture of CO and H_2 (Run 19). Conversely, when water was removed from the reaction by keeping the temperature of the cold finger substantially below the freezing point of water, the rate of formation of CO_2 was almost zero (Runs 21 and 22). This was also observed in the CO_2 - $^3H_2$ system[16] by the absence of a back reaction in CO_2 decompositions at low temperatures.

In Runs 23 and 26, the rate of formation of $C^{16}O_2$ from $C^{16}O$, in the presence of added $H_2{}^{18}O$, was approximately the same as in its absence, although the total rate of formation of CO_2 was increased because of the $C^{16}O^{18}O$ formed (Table III). This indicates that excess water does not increase the rate of radiolytic self-oxidation of CO.

Taken together, these results suggest that an oxygen-containing radical or ion, derivable from H_2O or CO with H_2, is the species responsible for oxidizing CO. The oxidant cannot be H_2O itself, because in Runs 23 and 26 the rate of reaction of $C^{16}O$ with $H_2{}^{18}O$ forming $C^{16}O^{18}O$ was of the same magnitude as the rate of formation of $C^{16}O$, whereas the concentration of $H_2{}^{18}O$ was many orders of magnitude greater than the trace concentrations of $H_2{}^{16}O$. It is also unlikely that the oxidant is atomic O. Although the matter has not been resolved, there is some evidence[27] that the reaction $O + CO + M \rightarrow CO_2 + M$ does not occur in the presence of H_2.

The primary oxidant for CO is almost certainly OH, as in Reaction (27). Evidence for this reaction is given by Reeves, Harteck, Thompson, and Waldron,[28] who employed it to explain their finding that the recombination of products of photolysis of CO_2 is catalized by H_2. Groth, Rommel and Schindler,[29] also employed Reaction (27) to explain the disappearance of CO during the photolysis of mixtures of CO_2 and H_2O. Reaction (27) competes with Reaction (26), and the rate constants[30,31] indicate that Reaction (26) predominates at low concentrations of CO.

A mechanism which is consistent with the mechanism postulated for formation of CH_4, and the rate law for formation of CO_2 (Eq. 32) may be derived as follows. Assuming that a steady-state pressure of OH exists, $R_{14} + R_{15}$ is equal to $R_{26} + R_{27}$, and the usual treatment yields

$$P_{OH} = \frac{(k_{14} + k_{15})\, P_{CO}\, P_{H_2}{}^*}{k_{26}\, P_{H_2} + k_{27}\, P_{CO}} \ . \tag{33}$$

Substituting this and Eq. (30) into R_{27} and $0.6\ R_{10}$ for R_{11} yields:

$$R_{27} = \frac{0.6\ R_{10}}{\left(1 + \frac{k_{26}}{k_{27}}\,\frac{P_{H_2}}{P_{CO}}\right)\left(1 + \frac{k_{13}}{k_{14} + k_{15}}\,\frac{P_{H_2}}{P_{CO}}\right)} \ . \tag{34}$$

The value for $k_{13}/(k_{14} + k_{15})$ of 0.051 obtained from the kinetics of CH_4 appearance, indicates that $k_{13}P_{H_2}/(k_{14} + k_{15})P_{CO} << 1$ and that Eq. (34) may be simplified to

$$\frac{R_{10}}{R_{27}} = \frac{k_{26}}{0.6\ k_{27}}\,\frac{P_{H_2}}{P_{CO}} + \frac{1}{0.6} \ . \tag{35}$$

This equation has the same form as Eq. (32), which gives a value for k_{26}/k_{27} of 0.30. The constants in the second terms of Eqs. (32) and (35) agree within the experimental error.

Literature values for the ratio k_{26}/k_{27}, at 23°C and with the isotope ^1H, are 0.030[30] and 0.051.[31] The isotope effect on this ratio is not known, although use of O^2H and $^2H_2$ decreased k_{26} and k_{27} by factors of 0.32[31] and 0.29[32] respectively. It is expected that use of ^3H in both reactions would increase the value of k_{26}/k_{27}. The experimental value of k_{26}/k_{27} may be high due to participation of the reaction, $H + OH + M \rightarrow H_2O + M$, possible errors in the value of 0.6 for the fraction of triplet $H_2{}^*$, and from the uncorrected isotope effect.

E. Exchange Reactions

In Runs 23 and 26, $C^{18}O$ was formed by reactions starting from $C^{16}O$ and $^3H_2{}^{18}O$. The rates of formation of $C^{18}O$ were proportional to the rates of ionization of H_2O and CO, but unrelated to the rates of ionization of H_2 (Tables I and III). Therefore, the mechanism of forming $C^{18}O$ may depend upon the radiolysis of either $H_2{}^{18}O$ or $C^{16}O$.

The radiolysis of H_2O vapor produces primarily OH and H radicals, with G(H) caused by recombination of H_2O^+ with electrons of 2.7 and G(H) caused by dissociation of excited H_2O of 4.9.[33] Exchange between ^{18}OH and CO^{16} or their ions is unlikely because of the rapid competing reaction leading to formation of CO_2. It is also unlikely that the exchange mechanism involves the dissociation of CO because yields of atomic C from the energy absorbed in CO are believed to be low in the presence of H_2. It is more probable that $C^{18}O$ is formed by direct exchange between excited $C^{16}O$ or $H_2{}^{18}O$ and the other species.

The $C^{16}O^{18}O$ formed in Runs 23 and 26 is also derived from $H_2{}^{18}O$. A mechanism of ionization and dissociative recombination of $H_2{}^{18}O$ followed by Reaction (27) is compatible with the proposed reactions. Since the rates of forming $C^{16}O^{18}$ are greater than the rates of ionization of $H_2{}^{18}O$ it is necessary to postulate that ^{18}OH is formed from either excited $H_2{}^{18}O$ or a combination of ionized and excited $H_2{}^{18}O$.

Both $C^{18}O$ and $C^{16}O^{18}O$ may be formed from the energy absorbed in $H_2{}^{18}O$. Using the above G(H) values for radiolysis of H_2O, the rates of formation of $H_2{}^{18}O^*$ are estimated to be 4.9/2.7 times as great as the rates of ionization, or 7.4 x 10^{-2} and 11.2 x 10^{-2} for Runs 23 and 26 respectively. The sums of the rates of ionization (Table I) and excitation are approximately equal to the sums of the rates of formation of products (Table III, line 3), in agreement with this postulated mechanism.

In Run 24, ^{16}O was exchanged in a mixture of $C^{18}O$ and $C^{16}O_2$. The observed rate of formation of $C^{16}O$ was slightly less than the rate of ionization of CO_2 (Table IV), which agrees with a mechanism of ionization and dissociative recombination of $C^{16}O_2$ to form $C^{16}O$ and ^{16}O, followed by exchange as follows:

$$^{16}O + C^{18}O \rightarrow C^{16}O + {}^{18}O \ . \tag{36}$$

(In Run 25, the initial rate of formation of $C^{16}O$ was subject to a large experimental error because of the low concentration.) Reaction (36) can be postulated because competing reactions are unlikely; i.e. direct combination of ground-state O and CO to form CO_2 is either very slow or nonexistent in the absence of a third body,[11] and the reaction $O + H_2 \rightarrow OH + H$ is known to be slow.[33]

F. Formaldehyde

The mass-spectral peak at m/e 31 observed in all runs could be a formaldehyde fragment or a parent peak of the formyl radical. It is believed to be the formyl radical because the parent peak for formaldehyde at m/e 34 was of relatively low intensity and was not growing. The CHO^+ ion was also observed from CO_2 in a glow discharge by Dawson and Tickner.[34] The mechanism of formation of the CHO radical and CH_2O is speculative, but Reactions (19) to (24) are exothermic and Reaction (21) has been shown to be fast.[35] The CHO^+ ion is relatively stable, so that its primary reaction is believed to be recombination with an electron by Reactions (22) and (24), resulting in either no net decomposition of CO or the formation of CH_2O. Once the concentration of H_2O vapor has become high enough, the following fast reaction[36] may also occur: $H_2O + CHO^+ \rightarrow H_3O + CO$.

G. Polymer

In most experiments the major product of decomposition of CO and $^3H_2$ was polymer. Polymer was also formed during decomposition of mixtures of CO_2 and $^3H_2$, but only after after appreciable quantities of the product CO were formed.[16] In the reverse reaction (the radiolysis of a mixture of CH_4, H_2O, and $^3H_2$) CO_2 and a very low concentration of CO were formed, but no polymer was visible. Thus the polymer can be formed from CO but not from either CO_2 or CH_4.

Previous work has shown that a polymer of C_3O_2 is formed in the radiolysis of pure CO,[7] but polyformaldehyde (also called polyoxymethylene) is formed in the radiolysis of mixtures of CO and $^3H_2$.[13]

There is considerable evidence that the initial polymer to be formed from mixtures of CO and $^3H_2$ is polyformaldehyde. The white color of the polymer indicates that it can be polyformaldehyde, but not polymerized C_3O_2, which is dark colored. In Run 29 the combined rapid appearance of turbidity and disappearance of CH_2O indicates that CH_2O will polymerize rapidly. Since only low concentration of CH_2O were observed during reactions between CO and $^3H_2$, it seems that CH_2O is formed and immediately polymerizes.

In the gas chromatographic analyses for H_2O, a peak having a retention time equal to that of CH_2O appeared on the leading edge of the water peak. The peak height reached a maximum approximately 4 hours after initiation, when the turbidity was also high. Since monomeric CH_2O was present only at low concentrations, it appears that this peak resulted from decomposition of the polyformaldehyde aerosol in the hot column of the gas chromatograph.

The initial rate of disappearance of CH_2O in Run 29 was much greater than the total rate of ion-pair formation (Table V), indicating that polymerization could have occurred by a condensation reaction. With increasing temperature the rate of polymerization of CH_2O decreases and eventually the reaction reverses,[37] which can explain the low rate of formation of polymer in Run 36 at 100°C.

The rapid appearance of turbidity during the first few hours after mixing CO and $^3H_2$ can be explained as homogeneous nucleation of polymer formed in the gas phase. It is possible that the initial polymerization of CH_2O is retarded until the concentration of H_2O becomes high enough to catalyze it.[37] Following nucleation, considerable growth of monodisperse particles occurs, as shown by the large increase in turbidity accompanied by higher-order Tyndall spectra,[17] and the subsequent sedimentation onto the bottom of the bulb. Thus, if aerosol particles are present, polymer apparently accumulates on only the surface of the particles.

In experiments with initial H_2O, (Runs 19, 23, and 26) no turbidity was observed, but loss of carbon from components in the gas phase and a slowly appearing opalscent film on the glass indicated that polymer was forming. Thus, in the presence of H_2O surface polymerization occurs.

The initial polymer reacts slowly with $^3H_2$ until most of the O and some of the C have been converted into H_2O and CH_4. The composition and insolubility of the final polymer indicate that it approximates cross-linked polymethylene.

H. Summary of Rates

The reactions which occur in mixtures of CO and H_2 during radiolysis are summarized in Fig. 5. The major products of decomposition are a polymer assumed to be polyformaldehyde, CH_4, and CO_2. The initial rate of decomposition of CO is equal to the sum of the initial rates of formation of CO_2, CH_4, and polymer.

For mixtures of CO and H_2 at ambient temperature, values of G(-CO) are 2 to 4, whereas for pure CO they are about 8. In pure CO the yield is considerably below that predicted upon the basis of Reaction (3).[7] In mixtures of CO and H_2 the yields are even less. The decreased rates of decomposition are explained on the basis that the energy absorbed in the CO does not contribute to the formation of CO_2 or CH_4, and possibly does not contribute to the formation of polymer. Only the energy absorbed in the H_2 contributes to the formation of CO_2 and CH_4.

The rates of formation of CH_4 and CO_2 are related to each other. At high concentrations of CO the rate of formation of CO_2 is greater than the rate of formation of CH_4. This occurs because OH, which will combine with CO, is generated by both Reactions (14) and (15) whereas the rate of formation of CH_4 is limited by the rate of Reaction (14).

As the concentration of CO is decreased, the rates of formation of both CO_2 and CH_4 decrease, CO_2 decreasing faster. At low concentrations of CO, the rate of formation of CO_2 is less than the rate of formation of CH_4 because Reaction (26) predominates over Reaction (27) under these conditions.

Addition of H_2O to the system increases the rate of formation of CO_2 by means of Reaction (27), with OH formed through ionization and dissociative recombination of H_2O.

ACKNOWLEDGMENTS

The author wishes to thank Dr. R. M. Alire, Dr. G. L. Schott, and Dr. W. M. Jones, of this Laboratory, Dr. C. Colmenares of Lawrence Radiation Laboratory, Livermore, California, and Professor A. W. Czanderna of Clarkson College of Technology, Potsdam, New York, for their comments, suggestions, and critical review of this work.

REFERENCES

1. S. C. Lind, Radiation Chemistry of Gases, (Reinhold Publishing Corporation, New York, 1961); P. S. Rudolph and S. C. Lind, J. Chem. Phys., 33, 705 (1960).
2. A. R. Anderson, Fundamental Processes in Radiation Chemistry, P. Ausloos, Ed., (Interscience, New York, 1968), p. 281.
3. S. C. Lind and D. C. Bardwell, J. Am. Chem. Soc., 47, 2675 (1925).
4. R. E. Woodley, General Electric Report, HW-31929 (May 1954).
5. W. R. Marsh and J. Wright, U. K. Atomic Energy Authority, AERE-R4198 (May 1964).
6. S. Dondes, P. Harteck, and H. von Weyssenhoff, Z. Naturforsch., A 19, 13 (1964).
7. A. R. Anderson, J. V. F. Best, and M. J. Willett, Trans. Faraday Soc., 62, 595 (1966).
8. A. R. Blake and K. E. Hodgson, J. Chem. Soc., A, 533 (1966).
9. C. Willis and C. Devillers, Chem. Phys. Letters (Netherlands), 2, 51 (1968).
10. J. P. Briggs and P. G. Clay, Nature, 217, 947 (1968); Int. J. Radiat. Phys. Chem., 1, 67 (1969).
11. D. L. Baulch, D. D. Drysdale, and A. C. Lloyd, O.S.T.I. Report No. 1, (May 1968).
12. S. S. Barton, S. T. Blake, R. J. Beardsmore, R. T. Perry, M. Daniel, and W. Newstead, J. Phys. Chem., 71, 4573 (1967).
13. D. L. Douglas, J. Chem. Phys., 23, 1558 (1955).
14. F. Moseley, A. E. Truswell, and C. D. Edwards, U. K. Atomic Energy Authority, AERE-R-2913, Harwell (1959).
15. B. M. Mikhailov, V. G. Kiseleve, and V. S. Bogdanov, Akad. Nauk SSR Izvest. Seri Khimi (Eng. Tr.), 1430 (1964).
16. W. H. Beattie, LA-4657 (June 1971).
17. D. Sinclair and V. K. LaMer, Chem. Rev., 44, 245 (1949).
18. F. F. Martinotti, M. J. Welch, and A. P. Wolf, Chem. Comm., 3, 115 (1968).
19. J. Dubrin, C. Mackay, M. L. Pandow, and R. Wolfgang, J. Inorg. Nucl. Chem., 26, 2113 (1964).
20. W. Brown, J. R. McNesby, and A. M. Bass, J. Chem. Phys., 46, 2071 (1967).
21. C. A. McDowell, Mass Spectrometry, (McGraw-Hill, New York, 1963), Table 13.1; R. N. Varney, Phys. Rev. Letters, 12, 559 (1960).
22. A. G. Coulter, R. C. G. Leckey, and G. S. Higginson, Comptes Rendus de la VI Conference International de les Phenomenes D'Ionisation dans le Gas, Paris, (July 1963), Vol. II, Ed., P. Hubert, p. 161.
23. S. W. Benson, The Foundations of Chemical Kinetics, (McGraw-Hill Book Company, New York, 1960), p. 317.
24. W. M. Jones, Los Alamos Scientific Laboratory, Private Communication, based upon data by S.J.B. Corrigan, J. Chem. Phys., 43, 4381 (1965); also see W. M. Jones, J. Chem. Phys., 47, 4675 (1967).
25. J. W. S. Jamieson, and G. R. Brown, Can. J. Chem., 42, 1638 (1964).
26. P. S. Rudolph, Radiation Chemistry, Vol. II, Advances in Chemistry Series 82, Amer. Chem. Soc., (1968), p. 101.
27. W. E. Kaskan and W. G. Browne, "Kinetics of the $H_2/CO/O_2$ System," General Electric Missile and Space Division Report, R-63-SD-848 (1964).
28. R. Reeves, Jr., P. Harteck, B. A. Thompson, and R. W. Waldron, J. Phys. Chem., 70, 1637 (1966).
29. W. E. Groth, H. J. Rommel, and R. N. Schindler, Z. Phys. Chem. (Frankfurt am Main), 62, 188 (1968).
30. G. Dixon-Lewis, W. E. Wilson, and A. A. Westenberg, J. Chem. Phys., 44, 2877 (1966).

31. N. R. Greiner, J. Chem. Phys., 46, 2797, 3389 (1967); 48, 1413 (1968); 51, 5049 (1969).

32. A. A. Westenberg and W. E. Wilson, J. Chem. Phys., 45, 338 (1966).

33. J. K. Thomas, Advan. Radiat. Chem., 1, 168 (1969).

34. P. H. Dawson and A. W. Tickner, Reference 22, p. 79.

35. D. P. Stevenson and D. O. Schissler, J. Chem. Phys., 23, 1353 (1955).

36. H. Pritchard and A. G. Harrison, J. Chem. Phys., 48, 5623 (1968).

37. J. F. Walker, Formaldehyde, Third Ed., (Reinhold, New York, 1964), pp. 37-38.

CM/fb:256(25)